

Research article

Andreas Müller*, Maik Riedl, Thomas Penzel, Hendrik Bonnemeier, Jürgen Kurths and Niels Wessel

Coupling analysis of transient cardiovascular dynamics

Abstract: The analysis of effects from coupling in and between systems is important in data-driven investigations as practiced in many scientific fields. It allows deeper insights into the mechanisms of interaction emerging among individual smaller systems when forming complex systems as in the human circulatory system. For systems featuring various regimes, usually only the epochs before and after a transition between different regimes are analyzed, although relevant information might be hidden within these transitions. Transient behavior of cardiovascular variables may emerge, on the one hand, from the recovery of the system after a severe disturbance or, on the other hand, from adaptive behavior throughout changes of states. It contains important information about the processes involved and the relations between state variables such as heart rate, blood pressure, and respiration. Therefore, we apply an ensemble approach to extend the method of symbolic coupling traces to time-variant coupling analysis. These new ensemble symbolic coupling traces are capable of determining coupling direction, strength, and time offset τ from transient dynamics in multivariate cardiovascular data. We use this method to analyze data recorded during an orthostatic test to reveal a transient structure that cannot be detected by classic methods.

Keywords: cardiovascular system; coupling analysis; ensembles; symbolic dynamics; transients.

***Corresponding author: Andreas Müller,** Cardiovascular Physics, Department of Physics, Humboldt-Universität zu Berlin, Robert-Koch-Platz 4, 10115 Berlin, Germany, Phone: +49-30-2093-99189, Fax: +49-30-2093-99188, E-mail: andreas.mueller@physik.hu-berlin.de

Maik Riedl, Jürgen Kurths and Niels Wessel: Department of Physics, Humboldt-Universität zu Berlin, Berlin, Germany

Thomas Penzel: Interdisciplinary Center of Sleep Medicine, Charité Berlin, Berlin, Germany

Hendrik Bonnemeier: University Medical Center Schleswig-Holstein, Campus Kiel, Kiel, Germany

Jürgen Kurths: Potsdam Institute for Climate Impact Research (PIK), Potsdam, Germany; and Institute for Complex Systems and Mathematical Biology, University of Aberdeen, Aberdeen AB24 3UE, UK

Introduction

Biological systems such as the human circulatory system are complex, usually consisting of several smaller subsystems. To gain deeper insights into the mechanisms of interaction between those subsystems, the analysis of couplings plays an important role, especially in data-driven investigations as practiced in many scientific fields [2, 5, 6, 9, 13, 14, 17]. Recent research projects in the fields of medicine and physiology are, e.g., focused on the connection between heart rate and blood pressure (e.g., baroreflex) [22], the correlation between cortical and subcortical activity regarding the differences of heart rate variability during different sleep stages, or on the interaction between heart rate and respiration [12, 25]. Data recorded for these purposes almost always display nonstationarities, nonlinearities, and intrinsic noise as well as measurement noise. Therefore, the analysis of these signals, especially the detection of coupling directions, is complicated. Different methods, starting from cross-correlation *via* mutual predictability to information theoretic approaches [7, 8, 10, 18–20, 23, 26–28], have been applied to physiological data. All these methods are more or less able to find the directions of the interactions. However, due to the nonstationarity and nonlinearity of the underlying processes in biosignals, the conclusions are not consistent across the different methods. Recently, new methods based on order pattern analysis have been developed to circumvent these problems [11, 16]. Order patterns result from a coarse graining (symbolization) of the data, e.g., according to the ranks of the amplitudes. This symbolic representation of successive amplitudes is less sensitive to nonstationarities.

However, for systems featuring various structurally different regimes, this approach is not enough. In this case, the different epochs are typically analyzed separately, although relevant information might be hidden within the transitions between the regimes. In the cardiovascular system, these transients may occur either by the

recovery of the system after a severe disturbance (e.g., apnea during sleep) or by the adaptive behavior of the system throughout changes of states (e.g., orthostatic tests or change of sleep stages). These transient regime shifts contain important information about the underlying processes involved and the relations between state variables such as heart rate and blood pressure. Therefore, the analysis of time-dependent couplings during these transient epochs is an important current research problem.

Recently, a new idea to handle this kind of data has been proposed, using an ensemble approach [1, 15, 32]. We use this approach to extend the method of symbolic coupling traces (SCT) [33]. In this work, we will introduce the new ensemble symbolic coupling traces (eSCT) measure and test its capabilities to determine the temporal changes in the three aspects (coupling direction, coupling strength, and occurring time lag) of transient dynamics in multivariate cardiovascular data.

Materials and methods

The SCT method was introduced by Wessel et al. [33] and has been successfully applied in the analysis of the cardiovascular regulation during sleep [31] and the effects of a therapy for patients with sleep apnea [21].

Suppose we either have a bivariate time series $\{\bar{x}(i)\}_{i=1,\dots,N}$, where a certain event takes place M times at time points $i=T_0^k$ ($k=1,\dots,M$), or that we have M equally sampled bivariate time series $\{\bar{x}_k(i_k)\}_{i_k=1,\dots,N_k}^{k=1,\dots,M}$, where in each of these one event occurs at time points $i_k=T_0^k$. To build the ensembles in order to apply the eSCT method, we first have to align the M events/time series in a way that $T_0^k=T_0\forall k$. In the following, we will regard this ensemble of aligned time series for a certain time range $\{\bar{x}_k(t)=x_k(t),y_k(t)\}_{t=T_0-c_1,\dots,T_0+c_2}^{k=1,\dots,M}$. Now we can transform

the one-dimensional time series $x_k(t)$ and $y_k(t)$ into symbol time series $s_x^k(t)$ and $s_y^k(t)$ according to

$$s_z^k(t)=\begin{cases} 1, z_k(t)\leq z_k(t+\theta) \\ 0, z_k(t)>z_k(t+\theta) \end{cases}, \quad (1)$$

where θ is the time delay between the values regarded for the symbolification process. Throughout this work, it is set to the sampling time (recorded data) or to $\theta=1$ (model data), i.e., successive values in the time series are regarded. The index $k=1,\dots,M$ describes the ensemble elements.

Using these symbol sequences, words $w_x^k(t)$ and $w_y^k(t)$ of a predetermined length l of successive symbols are formed, resulting in $d=2^l$ different possible words. The words are then taken to compute the time-dependent joint bivariate word distribution [4]:

$$p_{ij}(t,\tau)=P(w_x^k(t)=W_i;w_y^k(t+\tau)=W_j). \quad (2)$$

The variable $p_{ij}(t,\tau)$ describes the probability that the words W_i and W_j occur in the word sequences $w_x^k(t)$ and $w_y^k(t)$ at time point t exactly τ time steps apart. This probability is estimated by building a histogram for each time point t and each lag τ , thus averaging over all the ensemble elements k . The basic SCT concept, which is identical for SCT and eSCT, is illustrated in Figure 1. The time-dependent difference

$$\Delta T(t,\tau)=T(t,\tau)-\bar{T}(t,\tau)=\sum_{i=j} p_{ij}(t,\tau)-\sum_{i=1,2^l;j=2^l+1-i} p_{ij}(t,\tau) \quad (3)$$

describes the discrepancy between structurally symmetric and diametric parts of the time series of the different variables, when shifted τ time steps against each other. Through this difference, it is possible to assess the relative coupling strength and the dominant mutual behavior

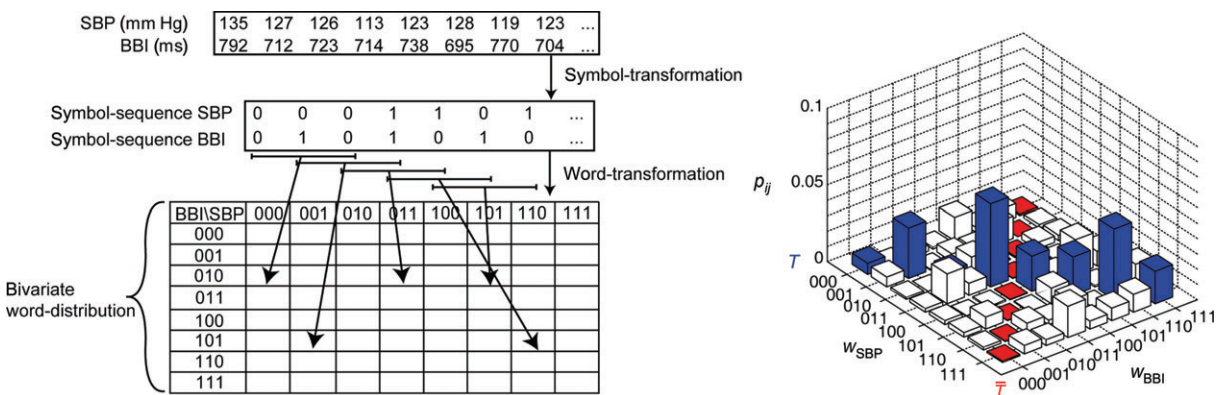


Figure 1 Illustration of the SCT [33].

After the symbolification of the time series, words of a certain length are formed and the bivariate word distribution is computed.

of both time series (symmetric or diametric). Using this difference has been shown to be more useful than using, e.g., Shannon entropy to characterize the $p_{ij}(t, \tau)$ matrix, as this just blurs the correct results. Using the corresponding values of τ , the coupling direction and the occurring time lag are determined. Using an empirical test [31], the significance of the resulting values can be assessed. In this method, the coupling direction is solely determined *via* the occurring time lags, which is sufficient for our purposes of developing descriptive models to help in predicting certain events, as we are only looking at causalities in the sense of Granger causality [10].

Using the symbolification approach, the amplitude information of the time series is lost. However, because this information can be quite unreliable due to noise, the SCT and eSCT methods are able to ignore random effects and concentrate on significant coupling information only. In Figure 2, five realizations of an AR process, described below, are shown, and the basic concept of the ensemble method in contrast to a time-averaging method is illustrated. In Figure 3, a representation of the results of the eSCT method applied on the data of the same AR process is shown and an explanation of how to read the diagram is given.

For a first test, we apply the eSCT on data generated by a simple AR model $x(i)=ax(i-1)+by(i-\tau_1(i))+\varepsilon_x(i)$, $y(i)=cy(i-1)+dy(i-\tau_2(i))+\varepsilon_y(i)$, where $a=c=0.3$ and $b=d=0.7$. In the first case, all model parameters were held constant throughout the simulation with $\tau_1=1$ and $\tau_2=2$ (Figure 4, upper panel). In the second case, the time lags τ_1 and τ_2 for the interactions between the two time series were changed at $i=200$ from $\tau_2=2$

to $\tau_2=5$ and at $i=700$ from $\tau_1=1$ to $\tau_1=3$ (Figure 4, lower panel). Further, we test the new method on data coming from two studies. From the first [21], we took the electrocardiogram (ECG) and blood pressure (systolic and diastolic) recordings from ten male control subjects during sleep. After identifying light sleep stages, as scored by qualified technicians, over all subjects, we were able to build an ensemble containing $M=152$ measurements of ECG and blood pressure, respectively, spanning a time of at least 18 beat-to-beat intervals. The time series are aligned at the beginning of the sleep stage as scored. From the second study [3], we took the ECG and blood pressure (also systolic and diastolic) recordings during an orthostatic test. The 346 subjects were first measured in a supine position, and then after a change of posture, in a standing position. For an initial test, we used the data from all subjects with no regard of age, gender, or body mass index to build an ensemble with a size of $M=346$ measurements. The ensemble time series are aligned using the event of standing up as scored in the data as the reference point and a time range of 110 beat-to-beat intervals before and after the event are regarded.

The time spans selected in these first tests represent a compromise between an ensemble that is as large as possible and a still representative time range.

Results

As a first step, we applied the eSCT on data generated by a simple AR model. Whereas the classic SCT (Figure 4A

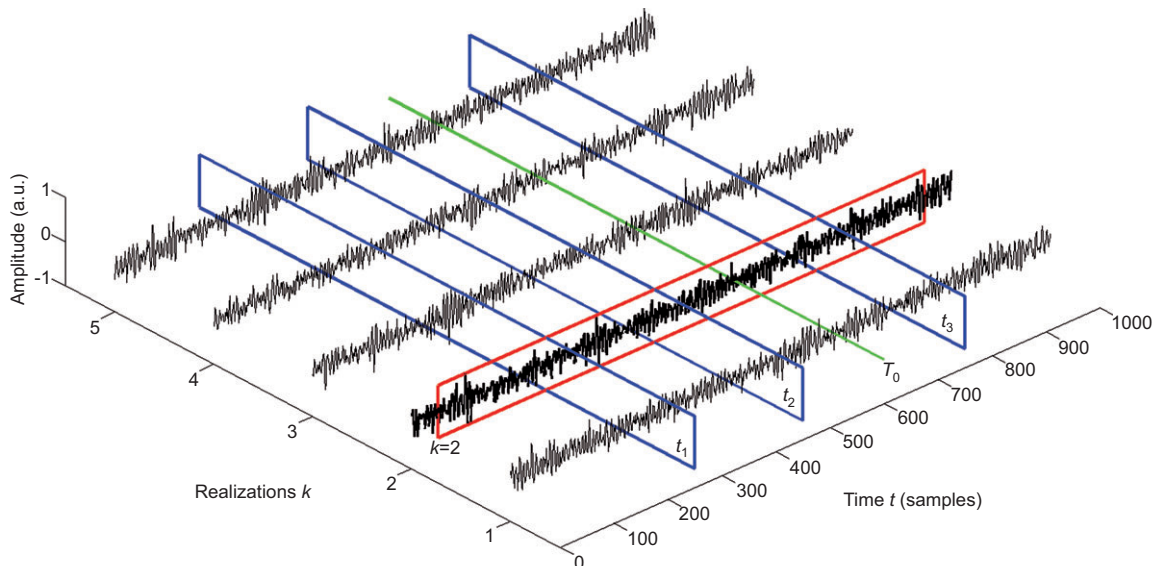


Figure 2 Illustration of the use of the ensemble approach for five realizations of an AR process.

The red rectangle shows the usual estimation over the time domain for the ensemble member $k=2$. The green line, labeled T_0 , shows the time point at which the ensemble time series are aligned. The blue rectangles show the estimation across the ensemble for three different time points.

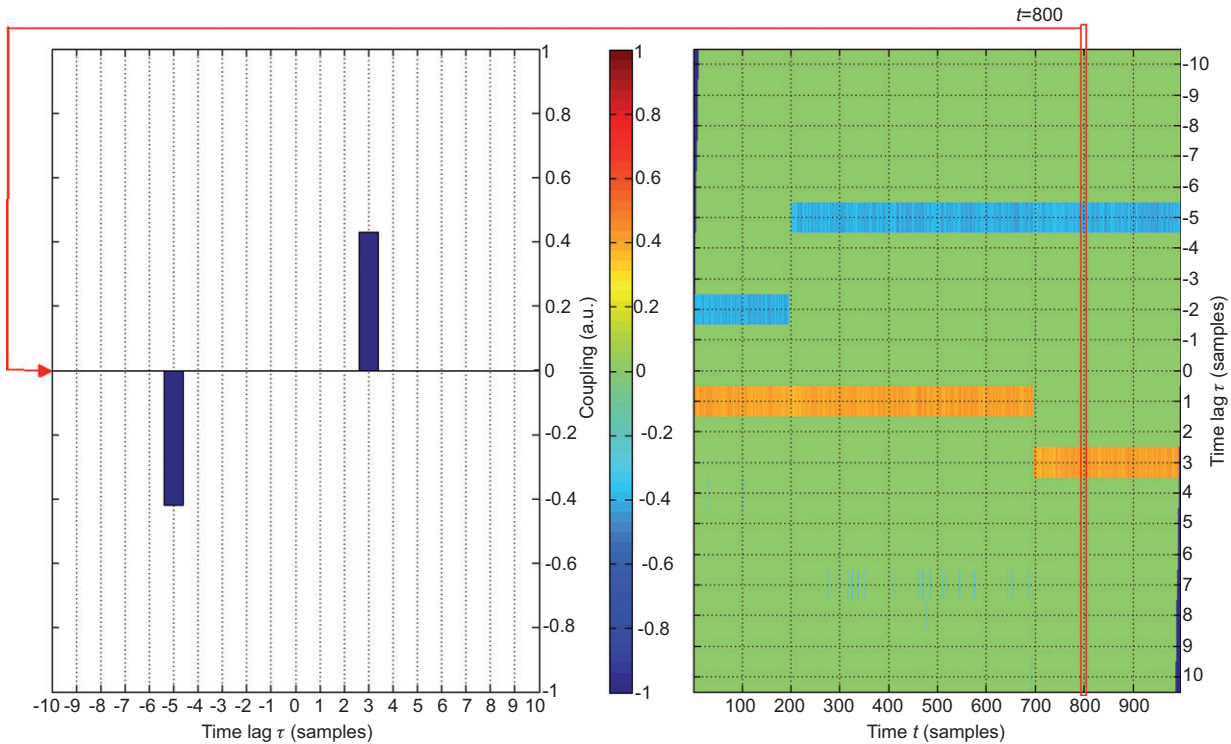


Figure 3 Representation of the results of the eSCT method applied to an AR process with time-varying parameters. The left panel shows a bar diagram (coupling strength over time lag) for time point $t=800$. Negative values in the coupling strength indicate diametric, whereas positive values represent symmetric coupling. The height of the bars corresponds to the color coding in the right panel, where the coupling strength for each time lag is plotted for each time point.

and B) only shows which time lag predominated over a larger time span, the eSCT (Figure 4C and D) shows the exact time points where the parameter changes occurred. The windowed cross-correlation (Figure 4E and F) also finds the correct lags but shows residues at other time lags and is not as accurate in identifying the time points where the switchings took place due to the length of the used window. In this test, an ensemble consisting of $M=1000$ realizations has been used to eliminate the effect of noise. In the case of this simple model data, the coupling structure can already be guessed using an ensemble size as small as $M=20$. Using $M=100$, the structure can already be clearly recognized with only little influences from noise. The dependency of the quality of the results on the ensemble size for this example is shown in Figure 5.

The next step was to test the eSCT on stationary heart rate and blood pressure data recorded during light sleep [21] in order to ascertain that the results obtained using the SCT method are reproduced. The results are shown in Figure 6. Both methods show significant couplings ($p < 0.01$) from diastolic to systolic blood pressure (symmetric, $\tau=1$), from beat-to-beat intervals to systolic blood pressure (diametric, $\tau=-2$), and instantaneous connections ($\tau=0$) between diastolic blood pressure and beat-to-beat

intervals (diametric) and between beat-to-beat intervals and systolic blood pressure (symmetric).

Finally, as a first test for the performance of the eSCT on transient data, we applied the method on blood pressure and beat-to-beat interval recordings (Figure 7) obtained during an orthostatic test [3]. The drastic changes in blood pressure and the almost complete disappearance of the respiratory sinus arrhythmia are clearly visible. In Figure 8, it can be seen that the regular structure (as seen in Figure 6) is disrupted during the event around time point $t=0$, where the subjects changed position. In the direct aftermath of the event, a growing symmetric influence of blood pressure on the beat-to-beat intervals can be observed. In the direct vicinity of the event, a gap appears in the $\tau=-2$ interaction. After the outburst around $t=20$, the regular structure is restored quite fast, although a lingering effect from blood pressure on the heart rate can be seen ($\tau=1$). Also, slight fluctuations in the coupling strength (fluctuations in the color), different from those before the event, are now present.

When compared with a windowed version of the SCT, the eSCT method shows clear advantages because of the tradeoff between window length and time resolution. Either the window length was too small for the SCT to

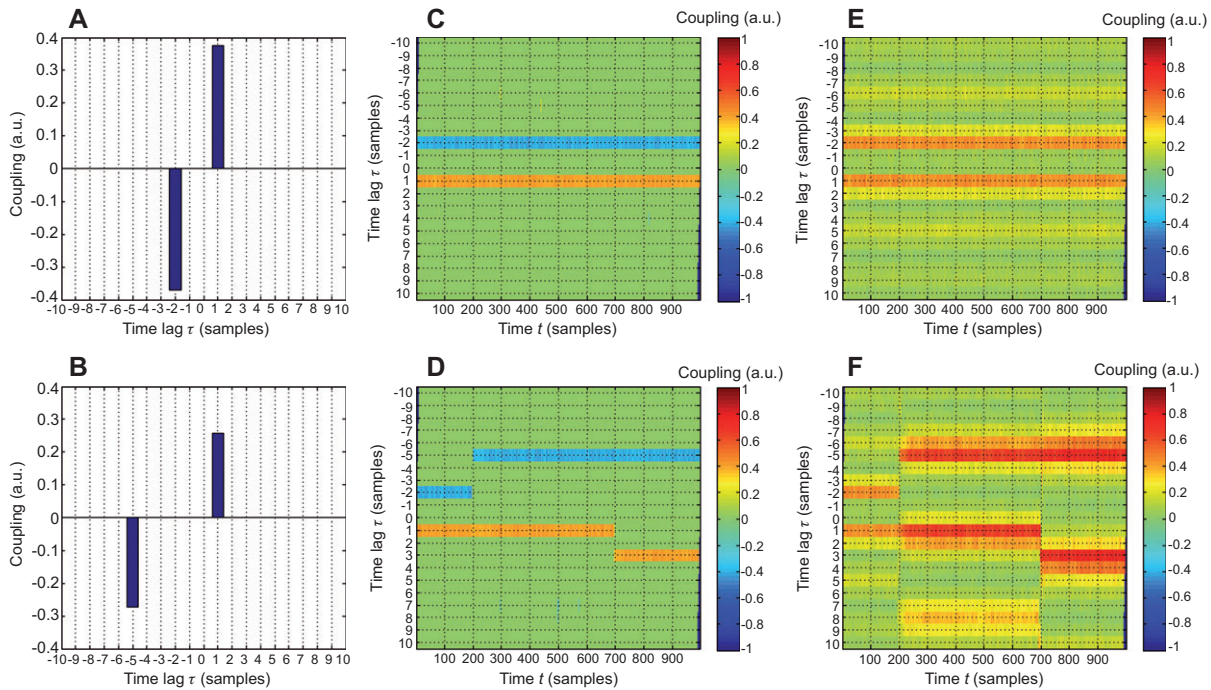


Figure 4 Comparison of the classic SCT and the eSCT method and the windowed cross-correlation (window length=100) for the AR model data. Time and time lags are shown as sample indices. In A, C, and E, all parameters and time lags stayed fixed throughout the simulation, and the first two methods detected the diametric coupling from x to y with time lag $\tau=-2$ and the symmetric coupling from y to x with time lag $\tau=1$. The windowed cross-correlation also identifies the correct time lags, although the results are more washed out and show a repetitive behavior for higher time lags. In B, D, and F, the occurring time lags have been switched at different time points. The SCT method (B) detects only the time lags that have been predominant over the longer period. The eSCT (D) detects the correct time lags, including the exact time points where the parameter changes took place. The windowed cross-correlation again shows the correct time lags and also some residue at other time lags, especially around the correct lags. Additionally, the time points where the parameter changes took place are not clearly identifiable due to the length of the used window.

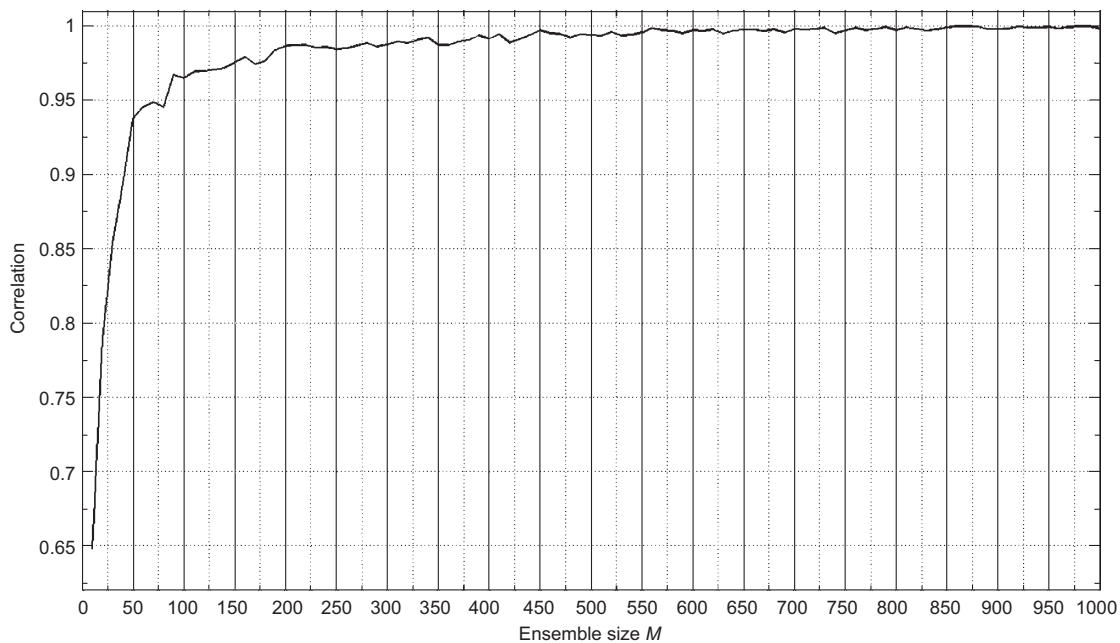


Figure 5 Dependency between the quality of the results and the ensemble size for the regarded AR process with time-varying parameters. The plot shows the mean correlation between the estimated coupling structure and the theoretic structure. For this simple example, the coupling structure can already be guessed for $M=20$ (correlation >0.75) and good results can be obtained for $M>90$ (correlation >0.95).

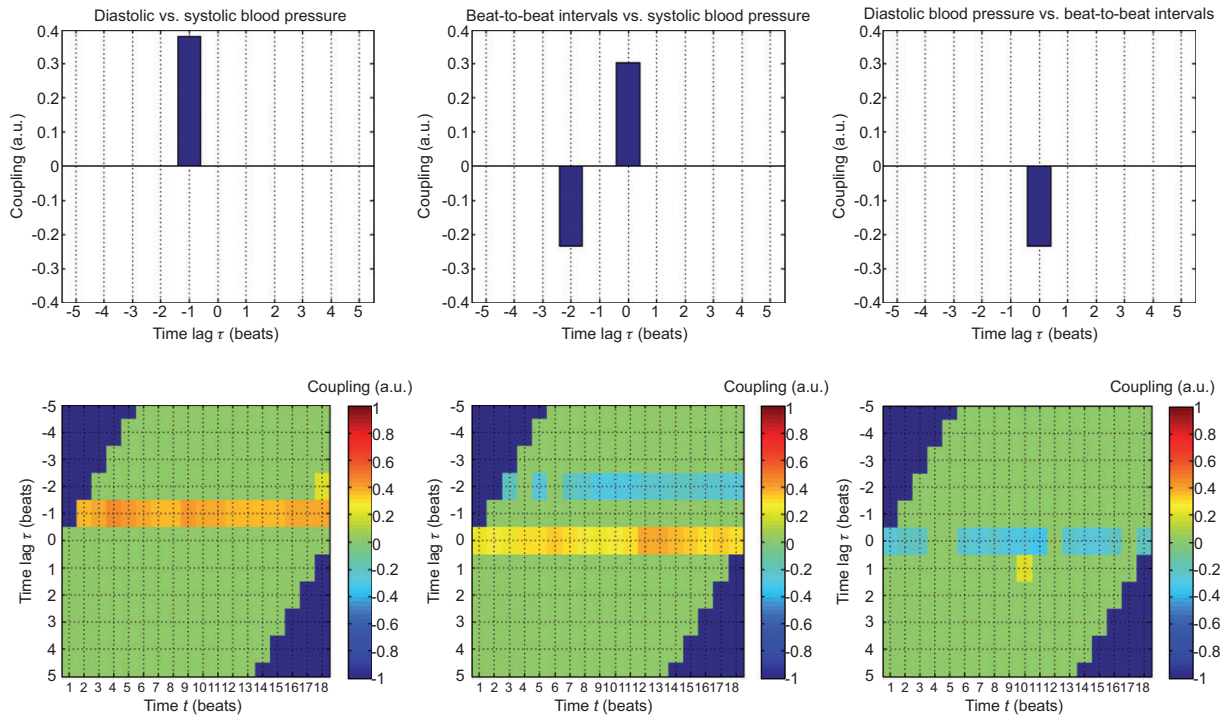


Figure 6 Comparison of the classic SCT and the eSCT method for stationary blood pressure and beat-to-beat intervals recorded during light sleep.

Time and time lags are shown as indices of the respective beat-to-beat intervals. Both methods detect the same time lags, relative coupling strengths, and the same mutual behavior of the time series. We find directional symmetric coupling from diastolic to systolic blood pressure (left, Frank-Starling mechanism) and diametric coupling from beat-to-beat intervals to systolic blood pressure (middle, baroreflex). The lag $\tau=0$ couplings represent mechanically induced arterial pressure fluctuations, e.g., due to respiratory movement.

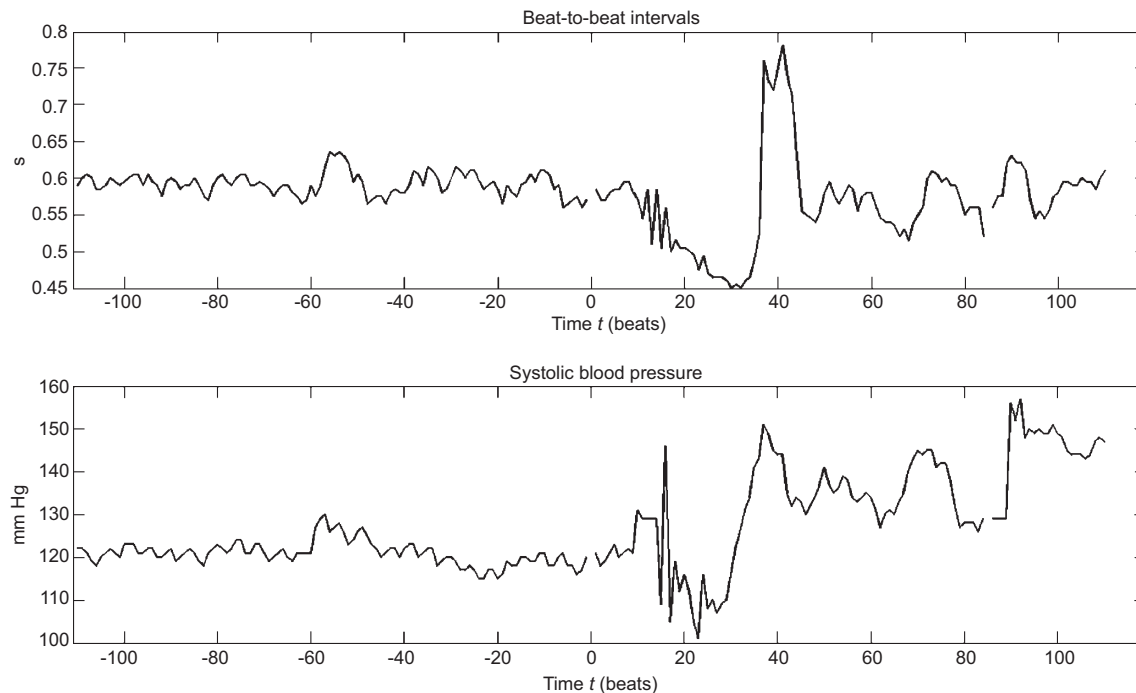


Figure 7 The time series of the systolic blood pressure and the interbeat intervals during an orthostatic test. Time and time lags are shown as indices of the respective beat-to-beat intervals. At time $t=0$, the change of posture took place. In the beginning of the event, the attenuation of the respiratory sinus arrhythmia can be seen.

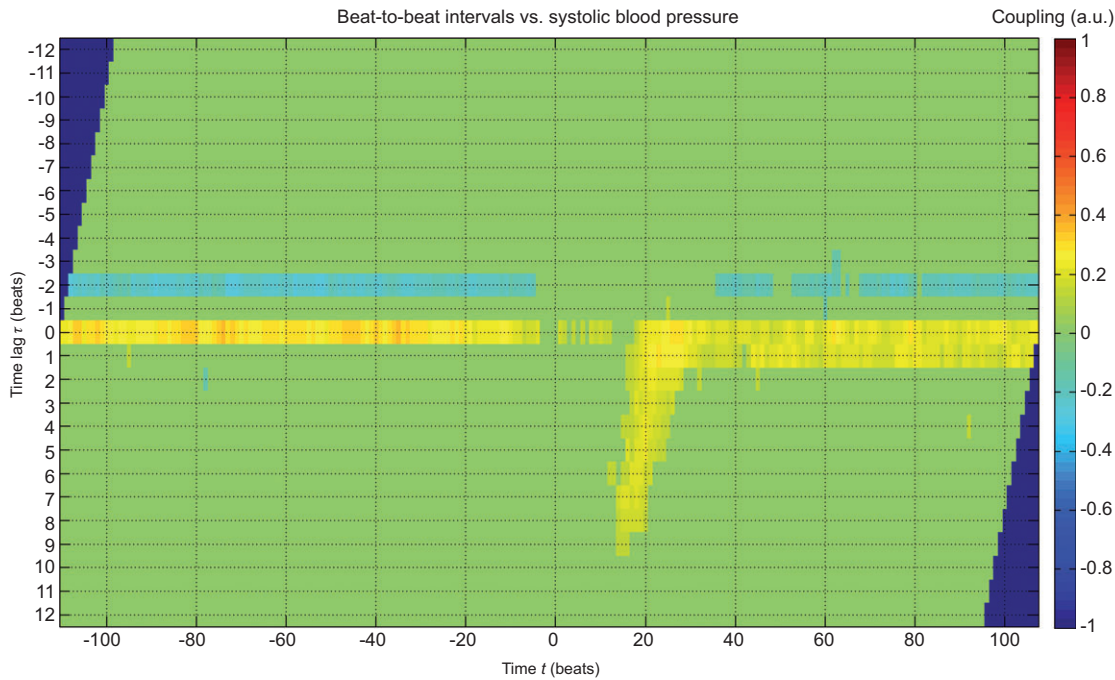


Figure 8 Results of the eSCT for systolic blood pressure and beat-to-beat interval recordings during an orthostatic test. Time and time lags are shown as indices of the respective beat-to-beat intervals. The regular structure (as seen in Figure 6) is disrupted during the event around time point $t=0$. In the direct aftermath of the event, a growing symmetric influence of blood pressure on the beat-to-beat intervals can be observed (baroreflex). After the outburst around $t=20$, the regular structure is restored quite fast, although a lingering effect from blood pressure on the heart rate can be seen ($\tau=1$).

show any meaningful results (noise) or too big to capture the transient event of the change of posture. We also compared the eSCT method with the windowed cross-correlation, but this time, no meaningful structure was discernible using the cross-correlation.

Discussion

The couplings found by applying our eSCT technique to real data confirm the predominating picture about cardiovascular short-term regulation. The significant connections found in the stationary data recorded during sleep (Figure 6) are from diastolic to systolic blood pressure (symmetric, $\tau=-1$), depicting the Frank-Starling mechanism due to the respiratory sinus arrhythmia [30], and from beat-to-beat intervals to systolic blood pressure (diametric, $\tau=-2$), illustrating the vagal feedback [33]. The lag $\tau=0$ connections between diastolic blood pressure and beat-to-beat intervals (diametric) and between beat-to-beat intervals and systolic blood pressure (symmetric) represent mechanically induced arterial pressure fluctuations due to respiratory movement [33].

The coupling structure found in the nonstationary data further corroborates the opinions about the

short-term regulation. The growing symmetric influence of blood pressure on the beat-to-beat intervals can be identified with the sympathetic baroreflex trying to compensate the drop in blood pressure. The gap in the $\tau=-2$ interaction between beat-to-beat intervals and blood pressure can be explained by the attenuated respiratory sinus arrhythmia (cf. Figure 7) and the strong dominance of the blood pressure drop at this time. The fluctuations in the coupling strength show an adapting process between blood pressure and heart rate, as the minima and maxima in the $\tau=0$ and $\tau=1$ region are alternating, indicating the presence of fast vagal and slower sympathetic controls.

The results of these first performance tests of the eSCT show promise for future applications of this method. We could show that our new method is indeed capable of detecting changes occurring in a complex system during transient behavior while reproducing the results of the classic method for stationary epochs. In a first application to a transient process, we were able to identify dynamical changes in coupling strength, direction, and occurring time lags in the baroreflex action. In all tests, the eSCT method outperformed the classic SCT measure and the windowed cross-correlation.

A couple of major challenges still have to be met in the future. The first one concerns the creation of suitable

ensembles, where two different cases need to be distinguished. One consists of the situations where certain events in one subject occur several times (e.g., event-related potentials, sleep arousals), allowing to build ensembles using similar events for each subject. In the other, more complicated case, there is one experiment performed on several subjects (e.g., orthostatic tests). Here the ensembles are built across the subjects. To do this, a reasonable grouping of the subjects has to be done, as different subjects will react differently in the same situation. In our first test, we did not perform such a grouping, but looked at all subjects together to get an ensemble that is as large as possible. The next step would be to look for differences in different groups, always keeping a minimal ensemble size in mind. Finally, we aim to develop an automated selection technique based on principal and independent component analysis, and similar methods.

The first results of our new method show a great potential to allow new insights into the short-term nonlinear cardiovascular regulation and to better predict potential health risks using the ensemble approach. Our next steps are to compare several coupling measures to select appropriate measures for transients and nonstationary physiological data, exploiting the generality of the ensemble approach, which permits us to use the scope of nonlinear, multivariate measures already developed. The coupling measures to be applied will be chosen from among well-known methods such as Granger causality [10], information theoretic techniques [20, 29], and others like in [24, 26] according to their suitability and performance.

Acknowledgment: This work was supported by the German Science Foundation (DFG WE2834/5-1).

Received November 14, 2012; accepted January 28, 2013; online first March 1, 2013

References

- [1] Andrzejak RG, Ledberg A, Deco G. Detecting event-related time-dependent directional couplings. *N J Phys* 2006; 8: 6.
- [2] Ashkenazy Y, Lewkowicz M, Levitan J, et al. Scale-specific and scale-independent measures of heart rate variability as risk indicators. *Eur Phys Lett* 2001; 53: 709–715.
- [3] Barantke M, Krauss T, Ortak J, et al. Effects of gender and aging on differential autonomic responses to orthostatic maneuvers. *J Cardiovasc Electrophysiol* 2008; 19: 1296–1303.
- [4] Baumert M, Walther T, Hopfe J, Stepan H, Faber R, Voss A. Joint symbolic dynamic analysis of beat-to-beat interactions of heart rate and systolic blood pressure in normal pregnancy. *Med Biol Eng Comput* 2002; 40: 241–245.
- [5] Blasius B, Huppert A, Stone L. Complex dynamics and phase synchronization in spatially extended ecological systems. *Nature* 1999; 399: 354–359.
- [6] Cammarota C, Rogora E. Spectral and symbolic analysis of heart rate data during the tilt test. *Phys Rev E* 2006; 74: 042903.
- [7] Dhamala M, Rangarajan G, Ding M. Estimating Granger causality from Fourier and wavelet transforms of time series data. *Phys Rev Lett* 2008; 100: 1–4.
- [8] Faes L, Cucino R, Nollo G. Mixed predictability and cross-validation to assess non-linear Granger causality in short cardiovascular variability series. *Biomed Eng* 2006; 51: 255–259.
- [9] Glass L. Synchronization and rhythmic processes in physiology. *Nature* 2001; 410: 277–284.
- [10] Granger CWJ. Investigating causal relations by econometric models and cross-spectral methods. *Econometrica* 1969; 37: 424–438.
- [11] Groth A. Visualization of coupling in time series by order recurrence plots. *Phys Rev E* 2005; 72: 1–8.
- [12] Hirsch JA, Bishop B. Respiratory sinus arrhythmia in humans: how breathing pattern modulates heart rate. *Am J Physiol* 1981; 241: H620–H629.
- [13] Ivanov PC, Nunes-Amaral LA, Goldberger AL, Stanley HE. Stochastic feedback and the regulation of biological rhythms. *Europhys Lett* 1998; 43: 363–368.
- [14] Lai Y-C, Kostelich EJ. Detectability of dynamical coupling from delay-coordinate embedding of scalar time series. *Phys Rev E* 2002; 66: 036217.
- [15] Martini M, Kranz TA, Wagner T, Lehnertz K. Inferring directional interactions from transient signals with symbolic transfer entropy. *Phys Rev E* 2011; 83: 011919.
- [16] Marwan N, Romano MC, Thiel M, Kurths J. Recurrence plots for the analysis of complex systems. *Phys Rep* 2007; 438: 5–6.
- [17] Milton JG, Cabrera JL, Ohira T. Unstable dynamical systems: delays, noise and control. *Eur Phys Lett* 2008; 83: 48001.
- [18] Müller M, Baier G, Rummel C, Schindler K. Estimating the strength of genuine and random correlations in non-stationary multivariate time series. *Europhys Lett* 2008; 84: 10009.
- [19] Nollo G, Faes L, Porta A, Antolini R, Ravelli F. Exploring directionality in spontaneous heart period and systolic pressure variability interactions in humans: implications in the evaluation of baroreflex gain. *Am J Physiol* 2005; 288: H1777–H1785.
- [20] Paluš M, Vejmelka M. Directionality of coupling from bivariate time series: how to avoid false causalities and missed connections. *Phys Rev E* 2007; 75: 1–14.
- [21] Penzel T, Riedl M, Gapelyuk A, et al. Effect of CPAP therapy on daytime cardiovascular regulations in patients with obstructive sleep apnea. *Comput Biol Med* 2012; 42: 328–34.
- [22] Porta A, Baselli G, Rimoldi O, Malliani A, Pagani M. Assessing baroreflex gain from spontaneous variability in conscious dogs: role of causality and respiration. *Am J Physiol Heart Circ Physiol* 2000; 279: 2558–2567.
- [23] Porta A, Furlan R, Rimoldi O, Pagani M, Malliani A, van de Borne P. Quantifying the strength of the linear causal coupling in closed loop interacting cardiovascular variability signals. *Biol Cybern* 2002; 86: 241–251.

- [24] Rosenblum MG, Pikovski AS. Detecting direction of coupling in interacting oscillators. *Phys Rev E* 2001; 64: 2–5.
- [25] Rosenblum MG, Kurths J, Pikovsky AS, Schäfer C, Tass PA, Abel H-H. Synchronization in noisy systems and cardiorespiratory interaction. *IEEE Eng Med Biol* 1998; 17: 46–53.
- [26] Rosenblum MG, Cimponeriu L, Bezerianos A, Patzak A, Mrowka R. Identification of coupling direction: application to cardiorespiratory interaction. *Phys Rev E* 2002; 65: 1–11.
- [27] Rummel C, Baier G, Müller M. Automated detection of time-dependent cross-correlation clusters in nonstationary time series. *Europhys Lett* 2007; 80: 68004.
- [28] Schelter BO, Winterhalder M, Dahlhaus R, Kurths J, Timmer J. Partial phase synchronization for multivariate synchronizing systems. *Phys Rev Lett* 2006; 96: 20.
- [29] Schreiber T. Measuring information transfer. *Phys Rev Lett* 2000; 85: 461–464.
- [30] Starling EH. *The Linacre lecture on the law of the heart*. London, UK: Longmans, Green and Co 1918.
- [31] Suhrbier A, Riedl M, Malberg H, et al. Cardiovascular regulation during sleep quantified by symbolic coupling traces. *Chaos* 2010; 20: 045124.
- [32] Wagner T, Fell J, Lehnertz K. The detection of transient directional couplings based on phase synchronization. *New J Phys* 2010; 12: 053031.
- [33] Wessel N, Suhrbier A, Riedl M, et al. Detection of time-delayed interactions in biosignals using symbolic coupling traces. *Europhys Lett* 2009; 87: 10004.